

Phase stability and elastic properties in the $\text{Al}_{1-x-y}\text{Cr}_x\text{Ti}_y\text{N}$ system from first principles

Erik Gutiérrez-Valladares ¹, Rurick Santos-Fragoso ^{1,2}, Guillermo Vázquez-Tovar ^{1,2}, Andrés Manuel Garay-Tapia ³, Diego Germán Espinosa-Arbeláez ¹, Raymundo Arróyave ⁴, Jesús González-Hernández ¹, Juan Manuel Alvarado-Orozco ¹

¹ Dirección de Ingeniería de Superficies, Centro de Ingeniería y Desarrollo Industrial, Querétaro, 76125, México.; egutierrez@posgrado.cidesi.edu.mx

² Facultad de Ingeniería, Universidad Autónoma de Querétaro, Querétaro, 76230, México

³ Centro de Investigación en Materiales Avanzados, Unidad Monterrey, 66600, Apodaca, Nuevo León, México.

⁴ Department of Materials Science and Engineering, Mechanical Engineering, Texas A&M University College of Engineering, College Station, Texas, USA.

Abstract

Multicomponent nitrides are a hot research topic in the search of hard coatings. The effect of substitutions on the phase stabilities, magnetic, and elastic properties of $\text{Al}_{1-x-y}\text{Cr}_x\text{Ti}_y\text{N}$ ($x,y=0-1$) was studied using first principles calculations based on the density functional theory. These calculations provide the lattice parameter, formation energy, mixing enthalpy and elastic constants. The calculated values are in good agreement with experiments and compare well with other theoretical results. A magnetic transition from antiferromagnetic to ferromagnetic state occurs at concentrations of B1-TiN higher than 60%. The quaternary zone has a lower aluminum solubility than the constituent ternary systems. The Poisson's ratio, Shear and Young modulus were used as predictors of the hardness, indicating that the higher hardness values are found on the transition line from B1 to B4. The obtained results enable the design of new $\text{Al}_{1-x-y}\text{Cr}_x\text{Ti}_y\text{N}$ -based materials for coating applications.

Keywords: ab initio study, elastic properties, phase stability, structural stability, spinodal decomposition, SQS.

1. Introduction

Transition metal nitrides have been widely used as protective coatings for machining, forging, and stamping applications due to their outstanding physical properties such as high hardness, chemical inertness, thermal stability, as well as oxidation and wear resistance [1, 2]. TiN and CrN coatings were an improvement compared to the traditional methods of heat treatment and nitriding, enhancing hardness to 28 and 20 GPa, and operating temperatures up to 550 and 700 °C, respectively [3].

CrN presents an antiferromagnetic behavior below the Néel temperature (~280 K) with an alternated spin double-layer configuration on an orthorhombic structure with $\alpha=88.23^\circ$ [4]. Above this temperature, CrN becomes paramagnetic with B1 structure [5]. The role of the magnetic contribution in Cr-containing systems is still an open research topic [6, 7, 8, 4, 9].

In order to improve the hardness, oxidation resistance, cutting performance, wear resistance, and the operating temperature more complex multicomponent nitrides have been studied. Particularly, it was discovered that by adding Al to TiN and CrN the above mentioned characteristics are improved [10, 11, 12, 13, 14, 15]. AlCrN and AlTiN are reported to be stable in the NaCl (B1) structure under an Al % at. composition—usually reported to be around 70%—, whereas at larger Al content occurs a transition to hexagonal (B4) structure which has a detrimental effect on the hardness of the coating [13, 16]. Comparing both ternary nitrides, AlCrN exhibits a slightly lower hardness than AlTiN at the same Al content [4]. However, Cr-based ternary

nitrides can dissolve a greater amount of Al in the B1 structure which retains the stability of the system to a higher temperature (925°C) [17]. In spite of Al having a strong influence on high temperature stability of the ternary nitrides, the Ti- and Cr-content grants the systems different degradation mechanisms. For AlCrN nucleation and growth is the main responsible for high temperature degradation (~1000°C); whereas for AlTiN the degradation mechanism (~900°C) is related to spinodal decomposition which involves the transformation of metastable cubic AlTiN zones into TiN-rich and AlN-rich zones [4, 18, 19].

Currently, there are plenty experimental and theoretical studies of AlCrN and AlTiN in which structural stability, mechanical properties, elastic constants, and magnetic behavior have been studied. However, only a few experimental and theoretical studies of CrTiN were found [7, 20]. CrTiN has lower hardness values across its different compositions compared to all other ternary nitride systems [21]. In spite of that drawback, the surprising magnetic behavior and the capacity of Cr and Ti to form protective oxide layers (Cr_2O_3 and TiO_2) are interest for electrical and corrosion protective applications [7, 22, 20, 23, 24].

Even though the previously discussed ternary systems are still an open research topic, the quaternary system $\text{Al}_{1-x-y}\text{Cr}_x\text{Ti}_y\text{N}$ has received attention due to the improvement of the cutting performance, hardness, and wear resistance at high temperature compared to the ternary nitrides. [25, 26, 27, 28]. Experimental studies have found that the oxidation resistance is negatively affected by Ti concentrations higher than 11 at. % due to the promotion of a TiO_2 porous surface layer over the more protective Al_2O_3 [28]. The pseudo-ternary AlCrTiN presents also a spinodal decomposition similar to AlTiN, where Cr is dis-

☆Pie de imagen

tributed into two metastable zones (AlCrN and TiCrN) resulting in an age hardening process [29]. Furthermore, Cr addition in the AlN phase decelerates the formation of the wurtzite phase, enhancing the thermal stability compared to the pseudo-binary TiAlN or CrAlN alloys [29, 30, 31].

Several experimental research focused on specific concentration points of this quaternary nitride can be found but only few theoretical studies focus on a full concentration range with emphasis on spinodal decomposition [31, 32, 33].

In this contribution, the Density Functional Theory (DFT) and the Special Quasirandom Structure (SQS) technique were employed to model $Al_{1-x-y}Cr_xTi_yN$ alloys. what makes this multicomponent nitride interesting is its chemical complexity and special rules must be followed for the atoms distribution into the lattice sites in order to represent the magnetic state. The study presents a complete calculation of a pseudo-ternary system using concentration steps of 12.5%. The configurations proposed in this study to simulate the magnetic effects are just an approximation of the most stable state. The stress-strain method was used to calculate the stiffness matrix on relaxed SQSs to accurately represent the alloy local effects [34, 35].

The aim of this paper is to study the quaternary nitride Al-CrTiN obtaining the Al solubility limit, elastic constants trends, phase stability, and second derivative of the mixing energy to observe the probability of spinodal decomposition.

2. Computational Methodology

The SQSs were made using the Alloy Theoretic Automated Toolkit (ATAT) software, which is based on the method proposed by Zunger *et al.*, for representing a valid model of $Al_{1-x-y}Cr_xTi_yN$ in a small supercell computationally feasible for DFT calculations [36, 37, 38]. The theoretical calculations are performed within the projector augmented wave (PAW) method and the density functional theory framework (DFT) as implemented in the Vienna ab-initio simulation package (VASP) [39, 40, 41, 42, 43, 44]. The electronic exchange-correlation potential is described within the generalized-gradient approximation (GGA) parametrized by Perdew *et al* [45]. The integration over the Brillouin zone employed the Monkhorst-Pack scheme using a grid of $5 \times 5 \times 5$ k-points for the B1 structures and a $9 \times 9 \times 4$ for the B4 structures [46]. An cut-off energy of 600eV was used for the calculations. The cells for both B1 and B4 structures went through a series of volume and ionic relaxations.

The Al solubility limit for B4 structures is expected to be above 50.0% Al. Therefore, for the B4 crystalline structures only concentrations above 50.0% Al were calculated, except for the AlCrN and AlTiN ternary nitrides in which all concentration points were studied.

Figure 1 shows the calculated compositions represented with circles. The grid consists of 45 concentration points with composition steps of 12.5 %, each point has a number label indicating which of the 9 generated SQSs was used.

The non-magnetic, ferromagnetic, and antiferromagnetic states at each concentration for the cubic and the hexagonal phases were calculated to find the most stable magnetic arrangement.

For the the Cr-containing points, the system was simulated as $Al_{1-x-y}Cr_xTi_yN$ $\uparrow Cr_xTi_yN$. Although an orthorhombic antiferromagnetic calculation was performed in the case of CrN, the reported states is the antiferromagnetic with Cr atoms arranged in an alternating spin single-layer configuration.

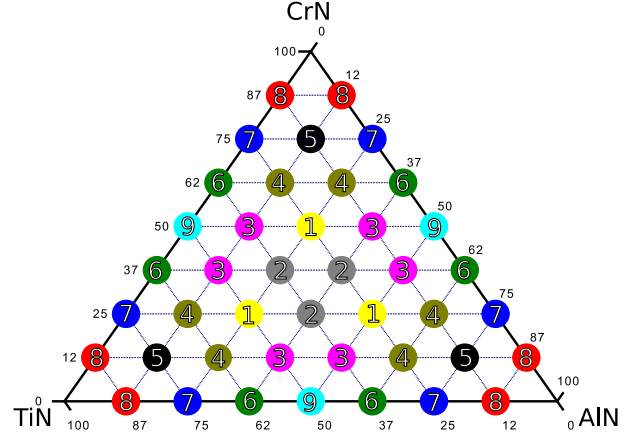


Figure 1: Phase Diagram of AlCrTiN

When the SQSs were relaxed, the total energy E (obtained from VASP) was compared against the most stable phases of each alloy component to obtain the formation enthalpy. For a quaternary nitride, the formation enthalpy ΔH_f is defined as

$$n\Delta H_f = E(Al_{1-x-y}Cr_xTi_yN) - (1-x-y)nE(Al) - xnE(Cr) - ynE(Ti) - (n/2)E(N_2) \quad (1)$$

In equation 1 the total energy of N was calculated for a N_2 molecule, while the total energies of Al, Cr and Ti were calculated for their unit cells in their respective stable structure.

Mixing Enthalpy ΔH_m of cubic $Al_{1-x-y}Cr_xTi_yN$ is defined as

$$n\Delta H_m = E(Al_{1-x-y}Cr_xTi_yN) - (1-x-y)(n/2)E(AlN) - x(n/2)E(CrN) - y(n/2)E(TiN) \quad (2)$$

In equation 2 the energies E of AlN, CrN and TiN are calculated in cubic phase.

2.1. Elastic Constants

The elastic constants were calculated using the stress-strain method [47, 48]. Positive and negative strains with a magnitude of $x = \pm 0.01$ were applied in all the strain tensor directions to modify the relaxed SQSs. Subsequently, the pseudo-inverse method to obtain the elastic constants values was applied and the stiffness tensor was calculated for the stable magnetic state of each SQS [48].

Since the point group symmetry is broken by the SQS approach, the elastic tensor matrix is symmetric and contains 21 values. The 9 non-zero values were averaged to obtain the macroscopic cubic elastic constants: $\overline{C}_{11} = (1/3)(C_{11} + C_{22} + C_{33})$, $\overline{C}_{12} = (1/3)(C_{12} + C_{13} + C_{23})$, $\overline{C}_{44} = (1/3)(C_{44} + C_{55} + C_{66})$ [49].

3. Results

3.1. Magnetic Stability

The magnetic properties of $\text{Al}_{1-x-y}\text{Cr}_x\text{Ti}_y\text{N}$ in the complete range of composition for the cubic phase and the hexagonal phase for Al content $> 50\%$ are shown in Figure 2a and 2b, respectively.

The TiN, AlN, and pseudo binary TiAlN do not exhibit magnetic behavior in any of the compositions of the cubic and hexagonal crystalline phases calculated [4]. As mentioned above, CrN presents an AFM behavior (below the Neel temperature) relating this with a distortion from cubic phase to the orthorhombic phase with a double layer arrangement [110]. In this study the AFM [100] arrangement is used to maintain the cubic phase [5].

The pseudo binary B1-AlCrN presents an AFM behavior in the complete range of compositions and B1-TiCrN exhibits a change in the magnetic behavior from FM to AFM. In this study due to the approximation used (GGA), the point B1-Ti₅₀Cr₅₀N presents an energy difference between the AFM and FM arrangements of 1 meV/atom making it difficult to determine the composition in which the transition takes place. According to Alling *et al.*, who use the LDA+U approximation, this change in the magnetic behavior occurs when there is approximately 50 at. content[7]. Because of this, the point B1-Ti₅₀Cr₅₀N is presented in the figure 4a as FM based on the observed tendency of the energy difference of the points B1-Ti_{62.5}Cr_{37.5}N and B1-Ti_{37.5}Cr_{62.5}N, which agrees with the magnetic transition reported by Alling *et al.*

For B1-Al_{1-x-y}Cr_xTi_yN a shift can also be observed in the magnetic behavior from AFM to FM. In the quaternary points studied, only the points where TiN $\leq 25\%$ at. content as well as Al₅₀Cr_{12.5}Ti_{37.5}N, and Al_{37.5}Cr_{12.5}Ti₅₀N present an AFM behavior. It is important to mention that the energy difference between the AF and AFM states of the Al_{12.5}Cr₅₀Ti_{37.5}N and Al₂₅Cr_{12.5}Ti_{62.5}N concentration points is similar to the difference in the B1-Ti₅₀Cr₅₀N point (1 meV/atom) making it difficult to determine the most stable magnetic state for these points, and the observed tendencies of the points are taken into account to determine the behavior represented in Figure 2a.

The points with CrN = 12.5% at. content may be influenced by the position of the two Cr atoms in the SQSs since, as reported by Filippetti *et al.* [50, 51], in the CrN the interactions (J) of the first neighbors have a negative value, favoring the AFM state while the interactions of second neighbors have a positive value favoring the FM state. This low CrN content can also explain the reason of the minimal energy difference between the FM and AFM states for the Al₂₅Cr_{12.5}Ti_{62.5}N.

Regarding the hexagonal phase, the pseudo binary B4-AlCrN presents a magnetic change from FM to AFM when there is CrN $\geq 63\%$ at. content (see Figure 2b) which is in agreement with previous reports [52, 53]. Likewise, for the quaternary B4-Al_{1-x-y}Cr_xTi_yN, the same magnetic shift was observed as in B4-AlCrN. The three quaternary points with Al=50% at. content and the point B4-Al_{62.5}Cr_{12.5}Ti₂₅N present an AFM behavior while the remaining points were FM.

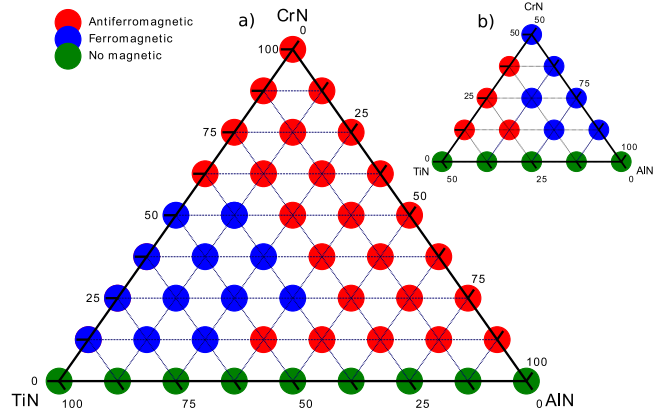


Figure 2: Magnetic Stability

3.2. Lattice Parameter

The lattice parameters were calculated from the relaxed SQSs shown in Figure 1; based on them, color map graphs were obtained by interpolation.

The Figure 3 shows, the lattice parameter variation for the cubic and hexagonal phases. The figure 2a is the ternary diagram for the cubic phase with its scale located at the left. The triangles in the right correspond to the lattice parameters of the hexagonal phase, figure 3b correspond to the parameter a with the scale located at the center and figure 3c to the parameter c with its scale located at the right.

The lattice parameter of the cubic phase increases almost as if it was only dependent on the Ti content. This may be promoted by the relatively big lattice parameter of TiN in comparison with the smaller lattice parameters of AlN and CrN. The same tendency in lattice parameter was found for the hexagonal phase where the maximum value for a and c was found at the TiN, while the minimum was located at the AlN point.

Even the lattice parameter change in the cubic phase for Al content higher than 50% has the same greater dependency on Cr content as the lattice parameters in the hexagonal phase have.

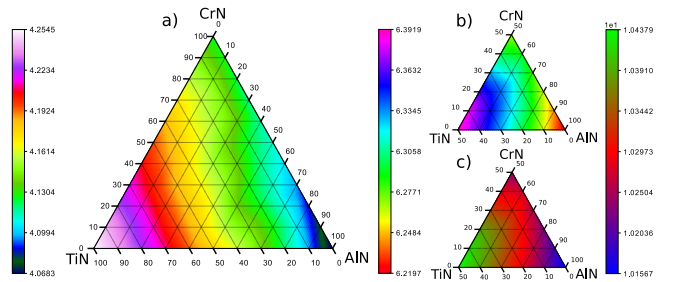


Figure 3: Lattice Parameter

3.3. Formation Enthalpy

The Formation Enthalpy for the cubic and hexagonal phase are presented in Figure 4a and 4b respectively, the equation 1 shows how the values for Formation Enthalpy were obtained.

The AFM B1-CrN presents the highest formation enthalpy value of the entire ternary diagram including the hexagonal phase (Figure 4b), the formation enthalpy obtained (-1.460 eV/at) is

in good agreement with the value reported by Mayrhofer *et al.* [[9]]. The B1-TiN presents the lowest formation enthalpy value of the entire ternary diagram and the AlN an intermediate value between the B1-CrN and B1-TiN.

For the pseudo binary nitrides B1-AlTiN and B1-CrAlN the obtained results are also in agreement with the values reported by Alling *et al.* and Mayrhofer *et al.*, for the case of B1-TiCrN no reported values were found, but it follows the trend of the other two pseudo binaries.

The formation enthalpy values of the quaternary nitride B1-AlTiCrN do not show a tendency established by any of the secondary nitrides, rather we can notice how the ternary diagram is divided into 3 zones, the corner of the TiN, the corner of the CrN and a zone that goes from the corner of the AlN to the line of the TiCrN nitride, the formation enthalpies of the B1-AlCrTiN are mainly in the middle of the scale values.

For B4-AlN as it was expected we obtain a lower formation enthalpy than B1-AlN, also it can be appreciated a change in the enthalpy minimum from the B1-TiN corner to the B4-AlN corner. The trends for the B4-AlCrTiN are not inclined to any of the secondary nitride, but with more B4-AlN content the B4 phase is more likely to be the most stable phase. And, if we maintain the Al and Ti content relation, more B4-CrN content means a higher formation energy. This behavior has found also in the B1 phase, only that B4 has a steepest ascent. Only comparing values from both formation energies we can calculate the Al solubility limit.

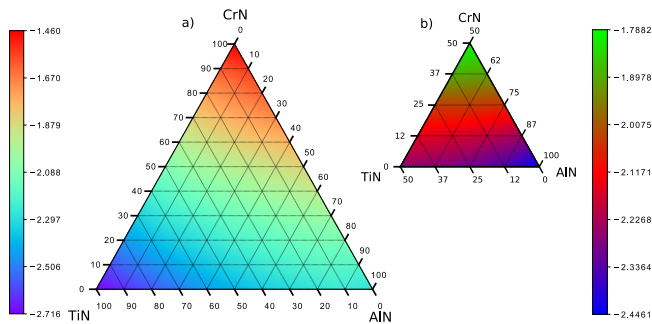


Figure 4: Formation Enthalpy

3.4. Phase stability

The formation energy of the cubic and hexagonal structures were plotted as 3D ternary surfaces in Figure 5, the intersection of both surfaces show where the cubic to the hexagonal transformation occurs. The projection shows the difference of formation energy between the cubic and the hexagonal phase $\Delta H_f = H_{f,cub} - H_{f,hex}$. The blue color in the Figure 5 shows the stable zone of cubic phase and the transition line point out the aluminium solubility limit. The aluminum solubility in the quaternary compositions is lower than the ternary nitrides (AlCrN, AlTiN).

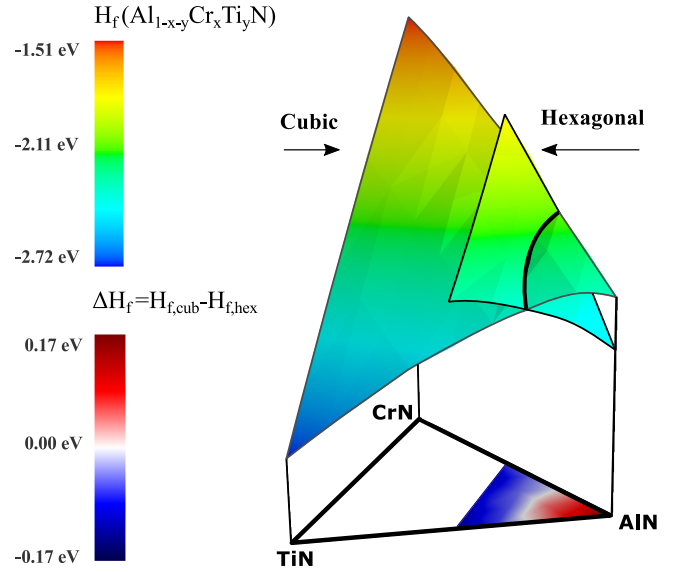


Figure 5: Phase Stability

3.5. Mixing Enthalpy

The Mixing Enthalpy for the cubic and hexagonal phase are presented in Figure 6a and 6b respectively. This values were obtained using the equation 2 explained in the section above. The ternary nitrides are in good agreement with the values previously reported by Alling *et al.* and Mayrhofer *et al.* [54, 4, 19] In Figure 6a it can be seen the same tendency found in the ternary nitrides, also a negative mixing enthalpy values can be found in the quaternary B1-AlCrTiN region near CrN suggesting a good stability. The B1-AlCrTiN section near the line of the B1-TiAlN is where the highest values of Mixing Enthalpy can be found, making this the most unstable region of the quaternary.

In general, B1-CrN content lowers the value of the Mixing Enthalpy. Considering only this chemical enthalpy, it means higher Cr content nitrides could have a greater thermal stability.

While B1-CrN content seems to considerably affect the Mixing Enthalpy, it only does if B1-AlN and B1-TiN content both are present in considerable amount. If not true, the enthalpy value does not vary in a noticeable way, maintaining an almost constant region in most of the B1-AlCrTiN mixing enthalpy, this being in agreement with the values reported by Lind *et al.* [31]

For B4-AlCrTiN it can be notice three evident regions shown in the figure 6b were the highest values can be found when there is more B4-CrN content. Only when there is more than 80% B4-AlN we can see an improvement in the B4 phase stability.

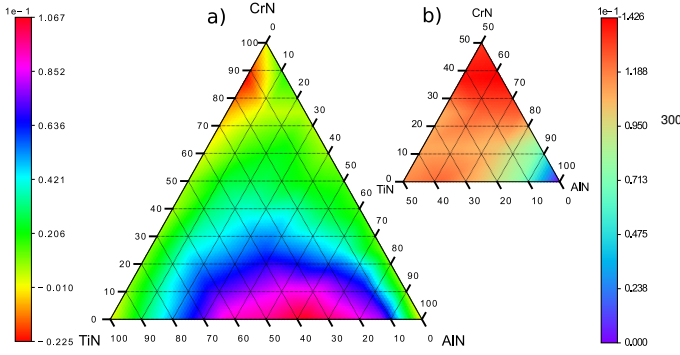


Figure 6: Mixing Enthalpy

3.6. Elastic Constants

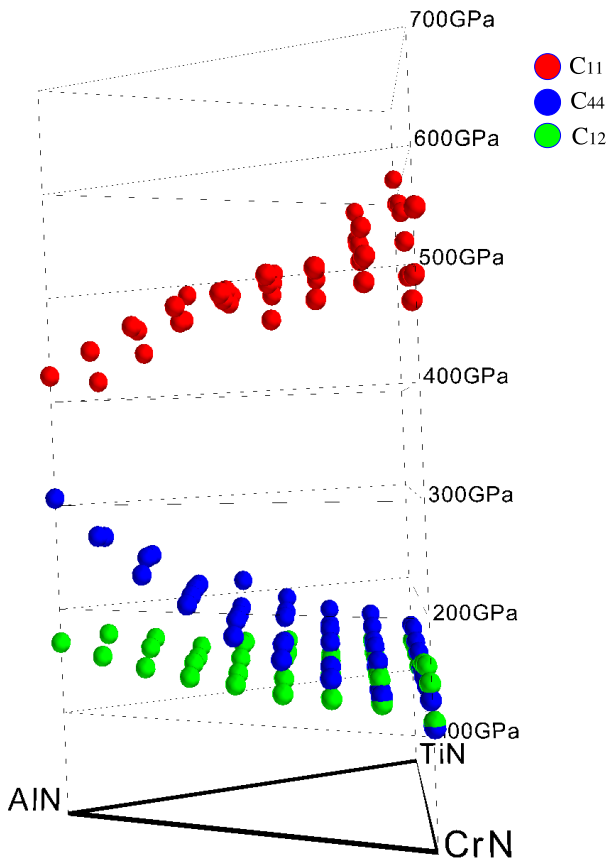


Figure 7: Elastic Constants

The elastic constants shown in fig. 7 show the three macroscopic elastic constants for the $Al_{1-x-y}Cr_xTi_yN$ alloy, C_{11} (red), C_{12} (green) and C_{44} (blue). The C_{11} constant has a maximum at the binary TiN, from this point the values of the ternary nitrides AlTiN and CrTiN have a negative slope reaching a minimum in points of low Ti concentration. This tendency is also present in the quaternary nitride. That is to say, low Ti concentration points show the smallest values in all the concentration region. Fixing the Ti content, the elastic constant magnitude increase with the Cr content. This is also true for AlCrN where a steady increase is present from AlN to CrN.

C_{44} is not affected by the variations of Cr and Ti content, by keeping the Al content fixed the slope of the resulting lines is close to zero. While increasing the aluminum content the elastic value grows rapidly and reaches its peak at the AlN point. C_{12} has the more straightforward trend of the 3 constants as it has practically the same value for all concentration points. The difference in the values obtained for the C_{12} constant are relatively small when are compared to the other elastic constants values. However, these results show similar tendencies to the ones presented in the C_{44} constant where the Al content is the most important variable for the elastic constant increment.

The Born stability criteria for the cubic system are the following conditions, which are necessary and sufficient to assert elastic stability [55]:

$$C_{11} - C_{12} > 0, \quad C_{11} + 2C_{12} > 0, \quad C_{44} > 0 \quad (3)$$

This criteria were calculated for all concentrations and were fulfilled by each one of them, showing that the structures are mechanically stable.

From the elastic tensor defined above, a number of derived properties are calculated [56, 57, 58].

Shear modulus Voigt average, G_V :

$$G_V = 15 (C_{11} - C_{12} + C_{44})$$

Shear modulus Reuss average, G_R

$$G_R = \frac{5C_{44}(C_{11} - C_{12})}{C_{44}}$$

Shear modulus average, G

$$2G = (G_V + G_R)$$

We may further obtain the the isotropic Young's modulus

$$E = \frac{9KG}{3K + G}$$

and the isotropic Poisson's ratio

$$\nu = \frac{3K - 2G}{2(3K + G)}$$

where $K = \frac{1}{3}(C_{11} + 2C_{12})$ and is the isotropic bulk modulus.

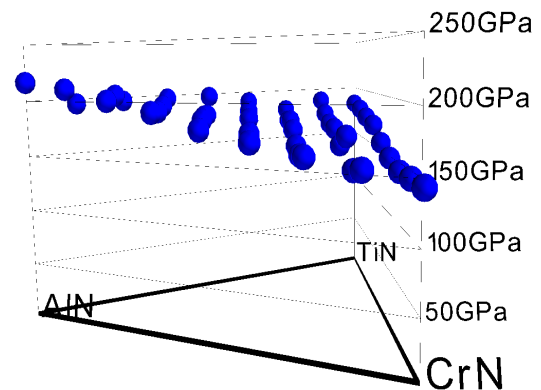


Figure 8: Shear Modulus Average Trends

Shear, Bulk and Young modulus have been used as empiric predictors of hardness in general [59, 60]. For cubic nitrides shear modulus, the inverse of Poisson's ratio and the ideal strength were found to have the biggest correlation values [58]. Considering this we analyze the tendencies of this constants in order to find a possible hardness tendency of the AlCrTiN system.

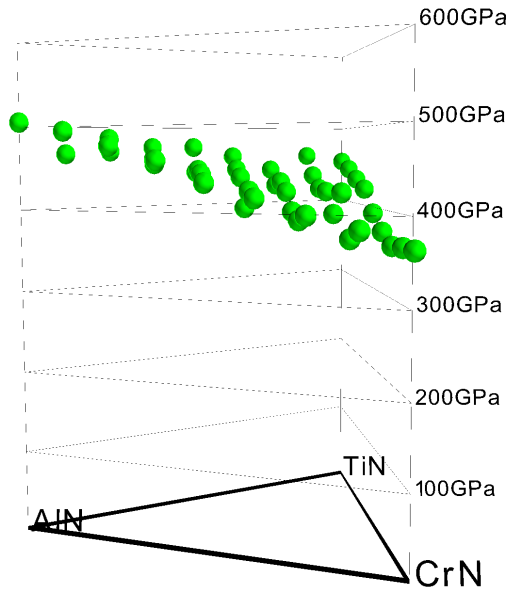


Figure 9: Young Modulus Trends

The shear modulus biggest influencing factor is C_{44} , and accordingly to what can be observed in figure 7 and 8 both grow as aluminum concentration increases, so being as close to as possible to AlN would give us the higher hardness values, however, we have to take into consideration the phase stability of the cubic phase as a limiting factor, showing that the higher hardness values would be found along the transition line between the B1 and B4 phases. The existence of this line with similar hardness values gives room to play with the quantities of Ti and Cr to also consider the phase stability and oxide resistance.

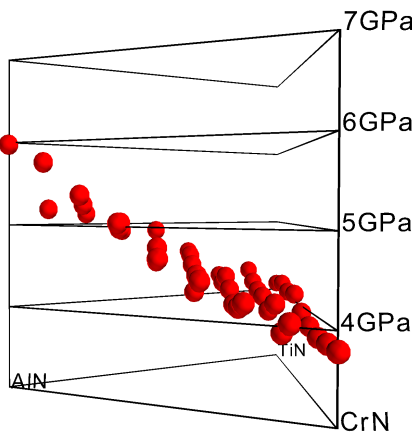


Figure 10: Poisson's Ratio Trends

4. Conclusions

A study of the $Al_{1-x-y}Cr_xTi_yN$ system in the pseudo-ternary concentration diagram ($0 \leq x \leq 1$ and $0 \leq y \leq 1$, with 12.5% x and y increments) was carried out. We found a good agreement between our calculations and the results of previously published studies for the formation energy, magnetic stability and elastic properties of the binary and ternary nitrides. These results allow us to ensure that the calculations of the quaternary region are a good approximation of the above-described characteristics.

The ternary nitrides present three different magnetic states (AFM, FM and NM), in the quaternary zone (AlCrTiN) two of this behaviors (AFM and FM) can be found as well as a change of behavior from AFM to FM when there is more than 60% of B1-TiN content. The results presented are a good approximation of the behavior of the system, but to improve the accuracy, calculations could be made with other approximations (LDA+U). For the B4-AlCrTiN the behavior present in figure 2b is in good agreement with the experimental results presented in previous studies [52, 53].

The stress-strain method was successfully used for the elastic constants calculus, all of these values are in the same range and followed characteristic trends in each constant. In this system, the approximated macroscopic elastic constants are of special importance as an aid to experimental design of materials. Since hardness can not be calculated directly from DFT calculations, we use the Poisson's ratio, Shear and Young Modulus to predict the hardness tendencies, which indicate that the higher hardness values for cubic are expected to be found along the transition line from B1 to B4 structure. According to the difference of formation energies there will be with a bit more aluminum solubility on the AlTiN side of the transition line, and the mixing energy shows a higher stability on the AlCrN side.

5. Acknowledgments

The authors are grateful with CONACYT for the financial support granted through the scholarship programs *Laboratorio Nacional de Proyección Térmica (293429)* and *Fronteras de la Ciencia (2015-02-1077)*, which made the development of the scientific activities reported possible.

References

- [1] S. Vepřek, The search for novel, superhard materials, *Journal of Vacuum Science & Technology A: Vacuum, Surfaces, and Films* 17 (5) (1999) 2401–2420. doi:10.1116/1.581977.
- [2] L. Hultman, Thermal stability of nitride thin films, *Vacuum* 57 (1) (2000) 1–30. doi:10.1016/S0042-207X(00)00143-3.
- [3] Y. Chim, X. Ding, X. Zeng, S. Zhang, Oxidation resistance of TiN, CrN, TiAlN and CrAlN coatings deposited by lateral rotating cathode arc, *Thin Solid Films* 517 (17) (2009) 4845–4849. doi:10.1016/j.tsf.2009.03.038.
- [4] B. Alling, T. Marten, I. a. Abrikosov, a. Karimi, Comparison of thermodynamic properties of cubic $Cr_{1-x}Al_xN$ and $Ti_{1-x}Al_xN$ from first-principles calculations, *Journal of Applied Physics* 102 (4). doi:10.1063/1.2773625.
- [5] L. M. Corliss, N. Elliott, J. M. Hastings, Antiferromagnetic structure of CrN, *Physical Review* 117 (4) (1960) 929–935. doi:10.1103/PhysRev.117.929.

- [6] P. Steneteg, B. Alling, I. a. Abrikosov, Equation of state of paramagnetic CrN from ab initio molecular dynamics, *Physical Review B* 85 (2012) 1–7. doi:10.1103/PhysRevB.85.144404.
- [7] B. Alling, Theory of the ferromagnetism in Ti_{1-x}Cr_xN solid solutions, *Physical Review B - Condensed Matter and Materials Physics* 82 (5). doi:10.1103/PhysRevB.82.054408.
- [8] B. Alling, L. Hultberg, L. Hultman, I. A. Abrikosov, Strong electron correlations stabilize paramagnetic cubic Cr_{1-x}Al_xN solid solutions, *Applied Physics Letters* 102 (3). doi:10.1063/1.4788747.
- [9] P. H. Mayrhofer, D. Music, T. Reeswinkel, H. G. Fuß, J. M. Schneider, Structure, elastic properties and phase stability of Cr_{1-x}Al_xN, *Acta Materialia* 56 (11) (2008) 2469–2475. doi:10.1016/j.actamat.2008.01.054.
- [10] H. Willmann, P. H. Mayrhofer, L. Hultman, C. Mitterer, Hardness evolution of AlCrN coatings under thermal load, *Journal of Materials Research* 23 (11) (2008) 2880–2885. doi:10.1557/JMR.2008.0366.
- [11] J. L. Endrino, G. S. Fox-Rabinovich, C. Gey, Hard AlTiN, AlCrN PVD coatings for machining of austenitic stainless steel, *Surface and Coatings Technology* 200 (24) (2006) 6840–6845. doi:10.1016/j.surfcoat.2005.10.030.
- [12] T. S. Kumar, S. B. Prabu, G. Manivasagam, K. a. Padmanabhan, Comparison of TiAlN, AlCrN, and AlCrN/TiAlN coatings for cutting-tool applications, *International Journal of Minerals, Metallurgy, and Materials* 21 (8) (2014) 796–805. doi:10.1007/s12613-014-0973-y.
- [13] A. E. Reiter, V. H. Derflinger, B. Hanselmann, T. Bachmann, B. Sartory, Investigation of the properties of Al_{1-x}Cr_xN coatings prepared by cathodic arc evaporation, *Surface and Coatings Technology* 200 (7) (2005) 2114–2122. doi:10.1016/j.surfcoat.2005.01.043.
- [14] K. Yamamoto, Properties of (Ti,Cr,Al)N coatings with high Al content deposited by new plasma enhanced arc-cathode, *Surface and Coatings Technology* 174–175 (2003) 620–626. doi:10.1016/S0257-8972(03)00580-2.
- [15] E. Schaffer, G. Kleer, Mechanical behavior of (Ti, Al) / N coatings exposed to elevated temperatures and an oxidative environment, *Surface & Coatings Technology* 133–134 (2000) 215–219.
- [16] B. Alling, a. V. Ruban, a. Karimi, L. Hultman, I. a. Abrikosov, Unified cluster expansion method applied to the configurational thermodynamics of cubic Ti_{1-x}Al_xN, *Physical Review B - Condensed Matter and Materials Physics* 83 (10) (2011) 1–21. doi:10.1103/PhysRevB.83.104203.
- [17] H. Willmann, P. Mayrhofer, P. Persson, A. Reiter, L. Hultman, C. Mitterer, Thermal stability of AlCrN hard coatings, *Scripta Materialia* 54 (11) (2006) 1847–1851. doi:10.1016/j.scriptamat.2006.02.023.
- [18] P. H. Mayrhofer, C. Mitterer, H. Clemens, Self-organized nanostructures in hard ceramic coatings, *Advanced Engineering Materials* 7 (12) (2005) 1071–1082. doi:10.1002/adem.200500154.
- [19] B. Alling, a. V. Ruban, A. Karimi, O. E. Peil, S. I. Simak, L. Hultman, I. a. Abrikosov, Mixing and decomposition thermodynamics of c-Ti_{1-x}Al_xN from first-principles calculations, *Physical Review B - Condensed Matter and Materials Physics* 75 (4) (2007) 1–13. doi:10.1103/PhysRevB.75.045123.
- [20] K. Inumaru, K. Koyama, Y. Miyaki, K. Tanaka, S. Yamanaka, Ferromagnetic Cr(x)Ti(1-x)N solid solution nitride thin films grown by pulsed laser deposition and their magnetoresistance, *Applied Physics Letters* 91 (15) (2007) 152501. doi:10.1063/1.2776853.
- [21] P. Hones, R. Sanjinés, F. Lévy, Sputter deposited chromium nitride based ternary compounds for hard coatings, *Thin Solid Films* 332 (1–2) (1998) 240–246. doi:10.1016/S0040-6090(98)00992-4.
- [22] H. S. Choi, D. H. Han, W. H. Hong, J. J. Lee, (Titanium, chromium) nitride coatings for bipolar plate of polymer electrolyte membrane fuel cell, *Journal of Power Sources* 189 (2) (2009) 966–971. doi:10.1016/j.jpowsour.2008.12.060.
- [23] K. Inumaru, Y. Miyaki, K. Tanaka, K. Koyama, S. Yamanaka, Magnetoresistance of ferromagnetic CrTiN solid solution nitride, *Physical Review B* 78 (5) (2008) 052406. doi:10.1103/PhysRevB.78.052406.
- [24] K. Inumaru, T. Ohara, K. Tanaka, S. Yamanaka, Layer-by-layer deposition of epitaxial TiN-CrN multilayers on MgO(0 0 1) by pulsed laser ablation, *Applied Surface Science* 235 (4) (2004) 460–464. doi:10.1016/j.apsusc.2004.03.260.
- [25] T. Polcar, A. Cavaleiro, Structure and tribological properties of Al-CrTiN coatings at elevated temperature, *Surface and Coatings Technology* 205 (SUPPL. 2) (2011) S107–S110. doi:10.1016/j.surfcoat.2011.03.015.
- [26] Y. Xu, L. Chen, Z. Liu, F. Pei, Y. Du, Influence of Ti on the mechanical properties, thermal stability and oxidation resistance of AlCrN coatings, *Vacuum* 120 (2015) 127–131. doi:10.1016/j.vacuum.2015.07.004.
- [27] J. L. Endrino, V. Derflinger, The influence of alloying elements on the phase stability and mechanical properties of AlCrN coatings, *Surface and Coatings Technology* 200 (1–4 SPEC. ISS.) (2005) 988–992. doi:10.1016/j.surfcoat.2005.02.196.
- [28] R. Forsén, M. P. Johansson, M. Odén, N. Ghafoor, Effects of Ti alloying of AlCrN coatings on thermal stability and oxidation resistance, *Thin Solid Films* 534 (534) (2013) 394–402. doi:10.1016/j.tsf.2013.03.003.
- [29] R. Forsén, M. Johansson, M. Odén, N. Ghafoor, Decomposition and phase transformation in TiCrAlN thin coatings, *Journal of Vacuum Science & Technology A: Vacuum, Surfaces, and Films* 30 (6) (2012) 061506. doi:10.1116/1.4757953.
- [30] H. W. Hugosson, H. Högberg, M. Algren, M. Rodmar, T. I. Selinder, Theory of the effects of substitutions on the phase stabilities of Ti_{1-x}Al_xN, *Journal of Applied Physics* 93 (8) (2003) 4505–4511. doi:10.1063/1.1557779.
- [31] H. Lind, R. Forsén, B. Alling, N. Ghafoor, F. Tasndi, M. P. Johansson, I. A. Abrikosov, M. Odén, Improving thermal stability of hard coating films via a concept of multicomponent alloying, *Applied Physics Letters* 99 (9). doi:10.1063/1.3631672.
- [32] Y. X. Xu, H. Riedl, D. Holec, L. Chen, Y. Du, P. H. Mayrhofer, Thermal stability and oxidation resistance of sputtered Ti[Al]Cr[N] hard coatings, *Surface and Coatings Technology* 324 (2017) 48–56. doi:10.1016/j.surfcoat.2017.05.053.
- [33] J. Zhou, L. Zhang, L. Chen, Effect of Cr on metastable phase equilibria and spinodal decomposition in c-TiAlN coatings: A CALPHAD and Cahn-Hilliard study, *Surface and Coatings Technology* 311 (2017) 231–237. doi:10.1016/j.surfcoat.2017.01.007.
- [34] D. Shin, R. Arróyave, Z. K. Liu, A. Van De Walle, Thermodynamic properties of binary hcp solution phases from special quasirandom structures, *Physical Review B - Condensed Matter and Materials Physics* 74 (2). doi:10.1103/PhysRevB.74.024204.
- [35] D. Shin, A. Van De Walle, Y. Wang, Z. K. Liu, First-principles study of ternary fcc solution phases from special quasirandom structures, *Physical Review B - Condensed Matter and Materials Physics* 76 (14) (2007) 1–10. doi:10.1103/PhysRevB.76.144204.
- [36] A. van de Walle, M. Asta, G. Ceder, The alloy theoretic automated toolkit: A user guide, *Calphad* 26 (4) (2002) 539–553. doi:10.1016/S0364-5916(02)80006-2.
- [37] A. van de Walle, Multicomponent multisublattice alloys, nonconfigurational entropy and other additions to the Alloy Theoretic Automated Toolkit, *Calphad: Computer Coupling of Phase Diagrams and Thermochemistry* 33 (2) (2009) 266–278. doi:10.1016/j.calphad.2008.12.005.
- [38] A. Zunger, S.-H. Wei, L. G. Ferreira, J. E. Bernard, Special quasirandom structures, *Physical Review Letters* 65 (3) (1990) 353–356. doi:10.1103/PhysRevLett.65.353.
- [39] P. E. Blöchl, Projector augmented-wave method, *Physical Review B* 50 (24) (1994) 17953–17979. doi:10.1103/PhysRevB.50.17953.
- [40] W. Kohn, L. J. Sham, Self-consistent equations including exchange and correlation effects, *Physical Review* 140 (4A). doi:10.1103/PhysRev.140.A1133.
- [41] R. O. Jones, O. Gunnarsson, The density functional formalism, its applications and prospects, *Reviews of Modern Physics* 61 (3) (1989) 689–746. doi:10.1103/RevModPhys.61.689.
- [42] G. Kresse, J. Hafner, Ab initio molecular dynamics for liquid metals, *Physical Review B* 47 (1) (1993) 558–561. doi:10.1103/PhysRevB.47.558.
- [43] G. Kresse, J. Furthmüller, Efficiency of ab-initio total energy calculations for metals and semiconductors using a plane-wave basis set, *Computational Materials Science* 6 (1) (1996) 15–50. doi:10.1016/0927-0256(96)00008-0.
- [44] G. Kresse, J. Furthmüller, Efficient iterative schemes for ab initio total-energy calculations using a plane-wave basis set, *Physical Review B - Condensed Matter and Materials Physics* 54 (16) (1996) 11169–11186. doi:10.1103/PhysRevB.54.11169.

- [45] J. D. Perdew, K. Burke, M. Ernzerhof, Generalized Gradient Approximation Made Simple, *Physical Review Letters* 77 (3) (1996) 3865–3868.
- [46] J. D. Pack, H. J. Monkhorst, "special points for Brillouin-zone integrations"-a reply, *Physical Review B* 16 (4) (1977) 1748–1749. doi:10.1103/PhysRevB.16.1748.
- [47] Y. Le Page, P. Saxe, Symmetry-general least-squares extraction of elastic data for strained materials from ab initio calculations of stress, *Physical Review B* 65 (10) (2002) 104104. doi:10.1103/PhysRevB.65.104104.
- [48] S. Shang, Y. Wang, Z. K. Liu, First-principles elastic constants of α - And θ - Al₂O₃, *Applied Physics Letters* 90 (10) (2007) 3–6. doi:10.1063/1.2711762.
- [49] M. Moakher, A. N. Norris, The closest elastic tensor of arbitrary symmetry to an elasticity tensor of lower symmetry, *Journal of Elasticity* 85 (3) (2006) 215–263. doi:10.1007/s10659-006-9082-0.
- [50] A. Filippetti, W. E. Pickett, B. M. Klein, Competition between Magnetic and Structural Transition in CrN (1998) 1–10 doi:10.1103/PhysRevB.59.7043.
- [51] A. Filippetti, N. A. Hill, Magnetic stress as a driving force of structural distortions: The case of CrN, *Physical Review Letters* 85 (24) (2000) 5166–5169. doi:10.1103/PhysRevLett.85.5166.
- [52] J. Zhang, X. Z. Li, B. Xu, D. J. Sellmyer, Influence of nitrogen growth pressure on the ferromagnetic properties of Cr-doped AlN thin films, *Applied Physics Letters* 86 (21) (2005) 1–3. doi:10.1063/1.1940131.
- [53] S. Y. Wu, H. X. Liu, L. Gu, R. K. Singh, L. Budd, M. van Schilfgaarde, M. R. McCartney, D. J. Smith, N. Newman, Synthesis, characterization, and modeling of high quality ferromagnetic Cr-doped AlN thin films, *Applied Physics Letters* 82 (18) (2003) 3047–3049. doi:10.1063/1.1570521.
- [54] P. H. Mayrhofer, D. Music, J. M. Schneider, Ab initio calculated binodal and spinodal of cubic Ti_{1-x}Al_xN, *Applied Physics Letters* 88 (7) (2006) 16–19. doi:10.1063/1.2177630.
- [55] F. Mouhat, F. Coudert, Necessary and Sufficient Elastic Stability Conditions in Various Crystal Systems, *Physical Review B* 90 (2014) 224104. doi:10.1103/PhysRevB.90.224104.
- [56] R. Hill, The Elastic Behaviour of a Crystalline Aggregate, *Proceedings of the Physical Society. Section A* 65 (5) (1952) 349–354. doi:10.1088/0370-1298/65/5/307.
- [57] Z. T. Y. Liu, X. Zhou, S. V. Khare, D. Gall, Structural, mechanical and electronic properties of 3d transition metal nitrides in cubic zincblende, rocksalt and cesium chloride structures: a first-principles investigation., *Journal of physics. Condensed matter : an Institute of Physics journal* 26 (2) (2014) 025404. doi:10.1088/0953-8984/26/2/025404.
- [58] B. D. Fulcher, X. Y. Cui, B. Delley, C. Stampfl, Hardness analysis of cubic metal mononitrides from first principles, *Physical Review B - Condensed Matter and Materials Physics* 85 (18) (2012) 1–9. doi:10.1103/PhysRevB.85.184106.
- [59] L. Zhou, D. Holec, P. H. Mayrhofer, First-principles study of elastic properties of cubic Cr_{1-x}Al_xN alloys, *Journal of Applied Physics* 113 (4) (2013) 043511. doi:10.1063/1.4789378.
- [60] J. Pokluda, M. Černý, M. Šob, Y. Umeno, Ab initio calculations of mechanical properties: Methods and applications, *Progress in Materials Science* 73 (2015) 127–158. doi:10.1016/j.pmatsci.2015.04.001.